Article ID: 1000-324X(2021)02-0217-08 **DOI:** 10.15541/jim20200231

Fabrication and Characterizations of Yb:YAG Transparent Ceramics Using Alcohol-water Co-precipitation Method

HUANG Xinyou[1], LIU Yumin[1,2], LIU Yang[3], LI Xiaoying[2,4], FENG Yagang[2,4], CHEN Xiaopu[2,4], CHEN Penghui[1,2], LIU Xin[2,4], XIE Tengfei[2,4], LI Jiang[2,4]

(1. School of Material Science and Engineering, Jiangsu University, Zhenjiang 212013, China; 2. Key Laboratory of Transparent Opto-functional Inorganic Materials, Shanghai Institute of Ceramics, Chinese Academy of Sciences, Shanghai 201899, China; 3. Science and Technology on Solid-State Laser Laboratory, North China Research Institute of Electro-Optics, Beijing 100015, China; 4. Center of Materials Science and Optoelectronic Engineering, University of Chinese Academy of Sciences, Beijing 100049, China)

Abstract: Yb^{3+} doped YAG transparent ceramics have great potential as gain medium for high-power solid-state lasers due to many advantages, such as broad absorption and emission bands, high gain, low thermal loading, long fluorescence lifetime and high quantum efficiency. So Yb:YAG transparent ceramics have gradually been paid more attention. In this work, we aimed at optimizing the properties of powders to fabricate highly transparent Yb:YAG ceramics. 5at%Yb:YAG nano-powders were synthesized *via* the co-precipitation method by using ammonium hydrogen carbonate as the precipitant, and pure water or alcohol-water mixture as the solvent. All powders calcined at 1250 ℃ for 4 h exhibit a pure YAG phase. Compared to the one with pure water solvent, the 5at%Yb:YAG powder synthesized with alcohol-water solvent exhibits smaller average crystallite size and lower agglomeration degree. 5at%Yb:YAG transparent ceramics were successfully fabricated by vacuum sintering without sintering additives from the obtained powder with alcohol-water solvent. The microstructure and in-line transmittance of the ceramics sintered at 1500–1825 ℃ for 20 h and 1800 ℃ for 10–50 h were investigated. All ceramic samples show a homogeneous microstructure except for that sintered at 1825 ℃ for 20 h. The sample sintered at 1800 ℃ for 50 h shows the highest in-line transmittance of 78.6% at 1100 nm and 76.7% at 400 nm (2.2 mm thickness). The calculated absorption and emission cross sections are 5.03×10^{-21} cm^2 at 937 nm and 13.48×10^{-21} cm^2 at 1031 nm, respectively. Therefore, Yb:YAG ceramics with high optical transparency and uniform microstructure have been fabricated from powder with alcohol-water solvent.

Key words: Yb:YAG transparent ceramic; alcohol-water co-precipitation; vacuum sintering; microstructure; optical property

Solid-state lasers have been widely used in manufacturing, medical science, laser weapons and other fields. The gain medium that generates laser by the stimulated radiation is essential component of solid-state lasers. Transparent ceramics have been widely investigated since Ikesue, *et al*[1] fabricated highly transparent Nd:YAG ceramics and firstly demonstrated them as a laser material in 1995. Compared with single crystals, polycrystalline transparent ceramics show shorter fabrication period, lower fabrication cost and higher doping concentration[2-4]. Transparent ceramics also exhibit superiorities over laser glass materials on thermal properties, laser monochromaticity and mechanical properties[5-8]. In the current laser application fields, compared with the leading competitor Nd:YAG ceramics, Yb:YAG transparent ceramics have no concentration quenching, significantly lower thermal loading, longer fluorescence lifetime and higher quantum efficiency[9], which make them one sort of the most pro-

Received date: 2020-04-29; **Revised date:** 2020-06-23; **Published online:** 2020-09-09
Foundation item: National Key R&D Program of China (2017YFB0310500); Key Research Project of the Frontier Science of the Chinese Academy of Sciences (QYZDB-SSW-JSC022)
Biography: HUANG Xinyou (1963–), male, professor. E-mail: huangxy@ujs.edu.cn
黄新友(1963–), 男, 教授. E-mail: huangxy@ujs.edu.cn
Corresponding author: LI Jiang, professor. E-mail: lijiang@mail.sic.ac.cn
李 江, 研究员. E-mail: lijiang@mail.sic.ac.cn

mising candidates for solid-state lasers.

There are two common methods employed to fabricate high-quality Yb:YAG transparent ceramics. One is solid-state reaction method, where the chemical reaction of commercial oxide powder mixtures happens during the sintering[10-14]. The other one is the non-reactive sintering of nanometer powders synthesized by wet-chemical methods[15-16]. Although solid-state reactive sintering is a relatively simple way to fabricate YAG-based transparent ceramics[17-22], it exhibits several disadvantages: inevitable impurities introduced from extensive ball milling and higher sintering temperature[23]. Compared to other wet-chemical methods such as Sol-Gel method[24], hydrothermal method[25], solvothermal method[26] and gel combustion[27], co-precipitation process[28-32] is a promising and effective way to synthesize YAG-based nano-powder with excellent chemical homogeneity and low synthesis temperature. These characteristics make the co-precipitation method very feasible to obtain YAG-based ceramics with appropriate microstructures and good optical properties. However, the traditional co-precipitation method commonly uses pure water as solvent, and the obtained powder show serious agglomeration degree. This makes it difficult to eliminate pores during the sintering, thereby decreasing the optical quality of ceramics[33-34]. Compared with the pure water, the distance between same molecules in the alcohol-water mixed solution is longer, which results in weaker hydrogen bonds between them. In addition, alcohol molecular has a steric effect which can prevent the precipitate particles from approaching. That is, the alcohol acts as the surfactant. In 2007, Tong, *et al*[35] firstly reported the pure-phase YAG powders prepared by alcohol-water co-precipitation method, and they found that alcohol can play the same role of the surfactant and contribute to the well-dispersion of the powder. In 2008, Tong, *et al*[36] reported that YAG powder synthesized by this method was sintered to transparent ceramics, and found that the powder obtained from alcohol-water solvent was more beneficial to preparation of high transparent ceramics than the powder derived from pure water solvent. In recent years, Chen, *et al*[37-38] also reported Yb:YAG transparent ceramics using alcohol-water co-precipitated powders, and the in-line transmittance of the obtained samples was above 83%. Briefly, using alcohol-water solvent is a very feasible method to reduce the agglomeration degree of the powder and further improve the optical quality of transparent ceramics.

In this work, 5at%Yb:YAG powders were synthesized by the co-precipitation method using pure water and alcohol-water mixture as the solvents, respectively. The phase composition and morphology of precursors and powders were discussed. The resultant 5at%Yb:YAG ceramics using alcohol-water co-precipitation method were obtained by vacuum sintering. The influence of sintering temperature and holding time on the microstructure and in-line transmittance of ceramics was systematically studied. The spectroscopic properties of the 5at%Yb:YAG ceramic sample with the highest in-line transmittance were also discussed.

1 Experimental

In the present work, nanosized 5at%Yb:YAG powders were synthesized by the co-precipitation method. The solutions of $Yb(NO_3)_3$ and $Y(NO_3)_3$ were prepared by dissolving Yb_2O_3 (99.995%, Changting Jinlong New Materials Co., Ltd., Fujian, China) and Y_2O_3 (99.99%, Yuelong New Materials Co., Ltd., Shanghai, China) in high-purity hot nitric acid, and $Al(NO_3)_3$ solution was obtained by dissolving $Al(NO_3)_3{\cdot}9H_2O$ (99.0%, Sinopharm Chemical Reagent Co., Ltd., China) in deionized water under stirring. According to the stoichiometric ratio of 5at%Yb:YAG ($Yb_{0.15}Y_{2.85}Al_5O_{12}$), the above nitrate solutions were mixed to obtain a solution of 0.48 mol/L for the metal ions. 0.0045 mol Yb^{3+}, 0.0855 mol Y^{3+} and 0.15 mol Al^{3+} present in the mixed solution. Precipitant solutions with a concentration of 1.5 mol/L were obtained by dissolving ammonium hydrogen carbonate (NH_4HCO_3) (99.995%, Aladdin, China) in the pure water and the alcohol-water solution mixed with a volume ratio of 1∶5, respectively. Ammonium sulfate ($(NH_4)_2SO_4$) (99.0%, Sinopharm Chemical Reagent Co., Ltd., China) was added into the precipitant solutions as the dispersant and the molar ratio of SO_4^{2-} to Al^{3+} was 1∶1. The mixed solutions of nitrate salts were then dripped at a rate of 20 mL/min into the precipitant solutions under stirring at room temperature. After aging for 1 h, the products were washed three times with deionized water and then three times with alcohol. The precursors were then dried at 70 ℃ for 36 h, sieved through 200-mesh (74 μm) screen and finally calcined in air at 1250 ℃ for 4 h to obtain the 5at%Yb:YAG nano-sized powders. After that, the powder synthesized by the alcohol-water co-precipitation method was uniaxially dry-pressed into pellets under 20 MPa and then cold isostatically pressed under 250 MPa. Sintering was conducted at 1500–1825 ℃ for 20 h and 1800 ℃ for 10–50 h in a vacuum furnace with tungsten heating elements. Finally, both surfaces of the ceramic samples were mirror-polished for subsequent testing.

The thermogravimetry and differential thermal analysis (TG-DTA) curves of the precursors were measured by a thermal analyzer (Thermoplus EVO II, Rigaku, Japan) at a heating rate of 10 ℃/min in the flowing air. Fourier transform infrared spectroscope (FT-IR) was performed on

an infrared spectrometer (Bruker VERTEX 70, Ettlingen, Germany) using the standard KBr method in the range of 4000–500 cm^{-1}. The phase composition of the precursors and powders was identified by the X-ray diffraction (XRD) (D/max 2200PC, Rigaku, Japan) with CuKα_1 radiation in the 2θ. The BET specific surface area of the powders was conducted by nitrogen adsorption *via* a Quantachrome instrument (Quadrasorb SI, Micromeritics, USA) at 77 K. The morphology of powders and the microstructure of ceramics were observed by a field emission scanning electron microscope (FESEM) (SU8220, Hitachi, Japan). The average grain size of ceramics was calculated using G=1.56L from the linear intercept method, where L is the average intercept length measured over 200 grains. The Archimedes method was used to measure the relative density of ceramics. The in-line transmittance of mirror-polished 5at%Yb:YAG ceramics was characterized by the UV-VIS-NIR spectrophotometer (Cary-5000, Varian, USA) in the wavelength range of 200–1100 nm.

2　Results and discussion

Fig. 1 shows the TG-DTA curves of the as-prepared precursors synthesized with pure water and alcohol-water solvents. It can be seen that the two TG-DTA curves are very similar, which indicates that the compositions of the two precursors are the same. The curves of the precursor synthesized with alcohol-water solvent were chosen for analysis. The curves show several stages of decomposition in the heating process with a total weight loss of 17.1%. The weight loss below 200 ℃ is mainly caused by the evaporation of adsorbed water and the decomposition of crystal water. The weight loss of this stage is about 9.4%, and a corresponding endothermic peak appears at 110 ℃. The broad endothermic band in the range of 200–900 ℃ is ascribed to the decomposition of carbonates and basic carbonate[39] with an approximate loss of 6.9%. The relatively sharper exothermic peak at 917 ℃ is associated with the formation of YAG phase. The broad endothermic peak at nearly 1001 ℃ can be related to the decomposition of sulfate, which is accompanied by 0.6% weight loss.

Fig. 2 shows the XRD patterns of the powders calcined at 1250 ℃ for 4 h synthesized with pure water and alcohol-water solvents. Diffraction peaks of the two powders are identified as the YAG phase (JCPDS 33-0040), and no diffraction peaks of intermediate phases appear. It indicates that the precursors have been completely transformed into the powders of pure YAG phase. The above shows that the composition of the two powders is nearly the same. The average crystallite sizes (D_{XRD}) of the 5at%Yb:YAG powders synthesized with pure water and alcohol-water solvents calcined at 1250 ℃ for 4 h are 84 and 65 nm, respectively, which were calculated using the Scherrer's formula:

$$D_{XRD} = 0.89\lambda / (\beta\cos\theta) \quad (1)$$

Where λ is the average wavelength of CuKα_1, β is the full width at half maximum (in 2θ), θ is the angle corresponding to the strongest peak. The average crystallite size of the powder synthesized with alcohol-water solvent is smaller, which may be explained by the Gibbs-Thomson equation:

$$\ln(c / c_s) = (2\sigma M) / (dRTr) \quad (2)$$

Where c is the actual concentration of the solution, c_s is the solubility of the solute, σ is the surface tension, M is the molar mass, d is the density of the crystal, T is the temperature, and r is the critical nucleation radius. The dielectric constant of the alcohol-water mixture is smaller than that of pure water at room temperature, which leads to a relatively lower solubility of solutes in the alcohol-water solvent. Then it can be seen from the equation that the critical nucleation radius of the powder with alcohol-water solvent should be smaller than that of the powder with pure water solvent.

Fig. 3 shows the FESEM micrographs of the precursors synthesized with pure water and alcohol-water

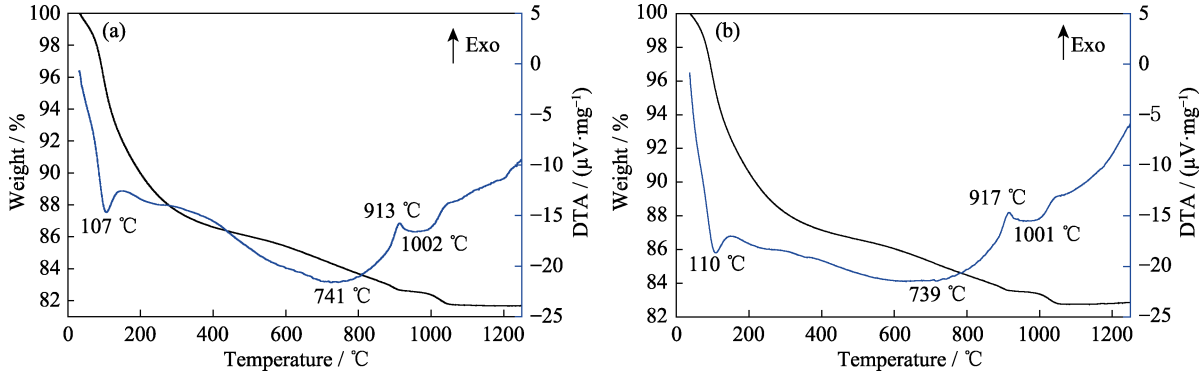

Fig. 1　TG-DTA curves of the as-prepared precursors synthesized with pure water (a) and alcohol-water (b) solvents

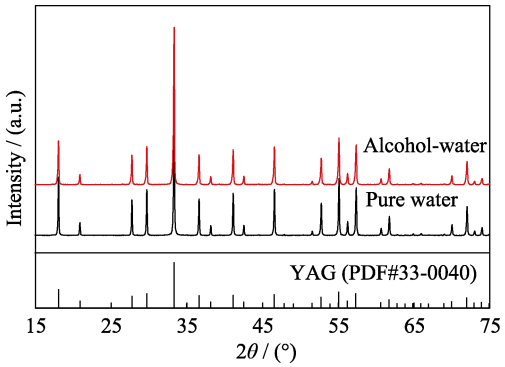

Fig. 2 XRD patterns of the powders calcined at 1250 ℃ for 4 h synthesized with pure water and alcohol-water solvents

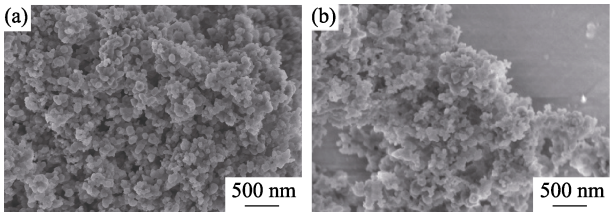

Fig. 3 FESEM micrographs of the as-synthesized precursors synthesized with pure water (a) and alcohol-water (b) solvents

solvents. It can be seen that the two precursors are mainly composed of agglomerated near-spherical particles.

Fig. 4 shows the FESEM micrographs of the 5at%Yb:YAG powders synthesized with pure water and alcohol-water solvents calcined at 1250 ℃ for 4 h. The two obtained 5at%Yb:YAG powders exhibit branch-like structure and a low degree of agglomeration. The agglomeration is related to the small particle size and high surface energy of the powder. The specific surface areas of the resultant powders synthesized with pure water and alcohol-water solvents are 7.398 and 9.683 m^2/g, respectively. The average particle size (D_{BET}) can be calculated by the following formula:

$$D_{BET} = 6/(\rho \cdot S_{BET}) \quad (3)$$

Where ρ is the theoretical density of 5at%Yb:YAG powder from the XRD (4.66 g/cm^3), S_{BET} is the specific surface area of the powder. The calculated average particle sizes of the 5at%Yb:YAG powders with pure water and alcohol-water solvents are 174 and 133 nm, respectively. The agglomeration coefficient can be calculated by the following formula:

$$N = (D_{BET}/D_{XRD})^3 \quad (4)$$

Where N is the agglomeration coefficient of powder. The calculated agglomeration coefficients of the 5at%Yb:YAG powders with pure water and alcohol-water solvents are 9.0 and 8.6, respectively. This indicates that the dispersity of the powder with alcohol-water solvent is better than that of the powder with pure water solvent. Therefore, 5at%Yb:YAG powder with alcohol-water solvent

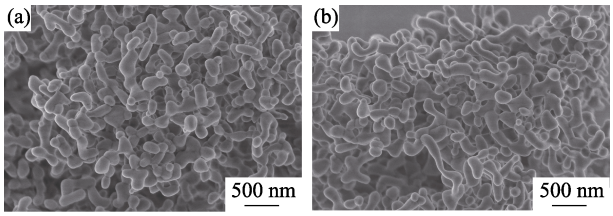

Fig. 4 FESEM micrographs of the 5at%Yb:YAG powders synthesized with pure water (a) and alcohol-water (b) solvents calcined at 1250 ℃ for 4 h

was used to fabricate the green bodies and ceramics in the following work.

The actual density of the green bodies was calculated by the geometric method. According to the theoretical density (4.66 g/cm^3) and actual density, the relative density of the green bodies is approximately 50%.

Fig. 5(a) shows the photographs of the polished 5at%Yb:YAG ceramic samples (2.2 mm thickness) sintered at 1500–1825 ℃ for 20 h. The in-line transmission curves corresponding to the transparent ceramics sintered at 1700–1825 ℃ for 20 h are shown in Fig. 5(b). It is noted that the ceramics sintered at 1500 ℃ and 1600 ℃ are completely opaque. The reason is the large number of large-sized residual pores inside the ceramic samples, which can be evidenced by the FESEM micrographs shown in Fig. 6(a) and (b). The ceramic sample sintered at 1700 ℃ starts to turn transparent, and the letters under the ceramic are clearly observed. With the further increase of sintering temperature, the in-line transmittance of ceramics increases steadily. The ceramic sample sintered at 1800 ℃ exhibits the highest value of 78.5% at 1100 nm and 76.7% at 400 nm, as shown in Fig. 5(b).

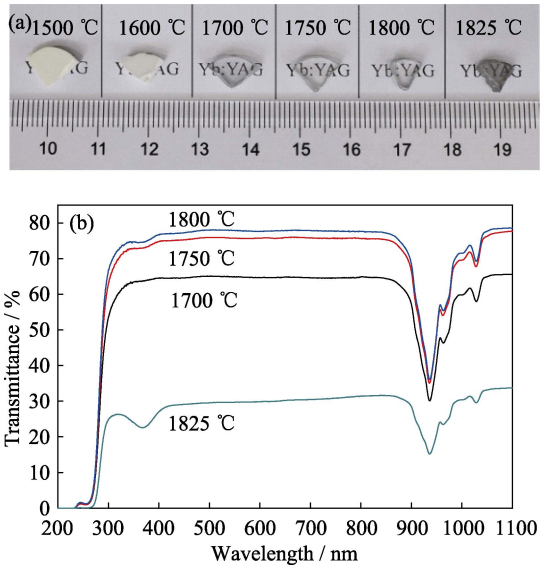

Fig. 5 Photographs (a) and in-line transmittances (b) of 5at%Yb:YAG ceramics (2.2 mm thickness) sintered at different temperatures for 20 h

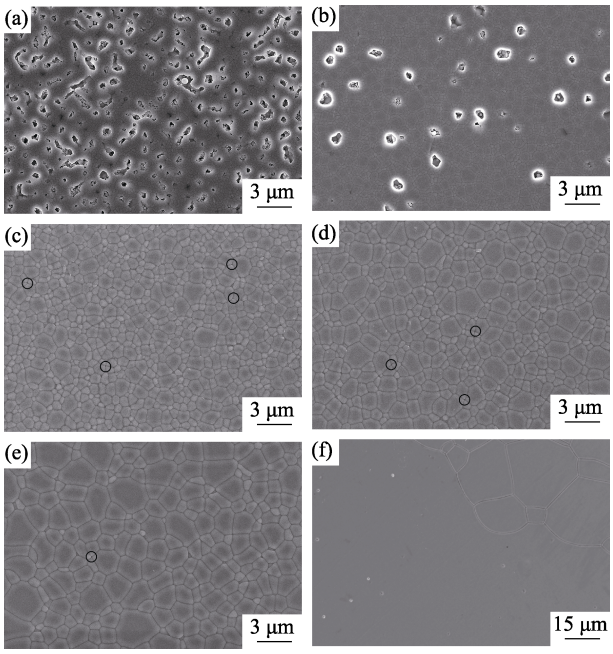

Fig. 6　FESEM micrographs of the thermally-etched surfaces of 5at%Yb:YAG ceramics sintered at various temperatures for 20 h

(a) 1500 ℃; (b) 1600 ℃; (c) 1700 ℃; (d) 1750 ℃; (e) 1800 ℃; (f) 1825 ℃

However, when the sintering temperature increases to 1825 ℃, the in-line transmittance of ceramic sample decreases significantly. It is worth mentioning that there are absorption bands near 380 nm in the transmission curves, which can be ascribed to the absorption of Yb^{2+}. This is consistent with the report of Singh, *et al*[40]. The volatilization of O^{2-} in the vacuum reducing atmosphere and the charge balance led to the generation of Yb^{2+}. The absorption band presented in the 240–260 nm region may be attributed to trace amounts of Fe^{3+} impurity ions[41].

Fig. 6 shows the FESEM micrographs of the 5at%Yb:YAG ceramics sintered at 1500–1825 ℃ for 20 h. As can be seen that the ceramic sample sintered at 1500 ℃ exhibits a large number of connected pores, and the average grain size is about 0.6 μm. When the sintering temperature increases from 1600 to 1700, 1750 and 1800 ℃, the average grain size increases from 0.9 to 1.2, 1.7 and 2.3 μm, respectively. For the ceramic sample sintered at 1825 ℃, abnormal grain growth appears, as shown in Fig. 6(f). When the sintering temperature is 1500, 1600, 1700, 1750 and 1800 ℃, the relative densities of ceramic samples are (83.6±0.1)%, (96.1±0.1)%, (99.4±0.2)%, (99.8±0.1)% and (99.9±0.1)%, respectively. However, for the ceramic sample sintered at 1825 ℃, the relative density decreases to (98.6±0.2)%. The reason is that the grain boundaries migrate too fast, which causes many pores trapped inside the grains. The above relative densities and average grain sizes of the 5at%Yb:YAG ceramics sintered at various temperatures for 20 h are shown in Fig. 7.

Fig. 8 shows the in-line transmission curves of the polished 5at%Yb:YAG ceramics (2.2 mm thickness) sintered at 1800 ℃ for various holding time. It is noted that all ceramics have high in-line transmittance, and the highest value is demonstrated by the sample sintered for 50 h. Specifically, this ceramic sample shows the in-line transmittance of 78.6% at 1100 nm and 76.7% at 400 nm. However, the in-line transmittance of the sample sintered for 20 h is similar to that of the sample sintered for 50 h.

Fig. 9 shows the microstructures of thermally etched surfaces of the 5at%Yb:YAG ceramics sintered at 1800 ℃ for various holding time. It can be found that the grain size of ceramics increases with the holding time prolonging, and all ceramic samples exhibit a homogeneous microstructure. The average grain sizes of ceramics sintered for 10, 20 and 50 h are 2.0, 2.3 and 3.7 μm, respectively. The residual pores in ceramics sintered for 20 and 50 h are less than those in the sample sintered for 10 h. The distribution of residual pores in 5at%Yb:YAG ceramics sintered for 20 and 50 h is similar, indicating that the influence of holding time over 20 h on promoting pores elimination is not obvious. This result is consistent

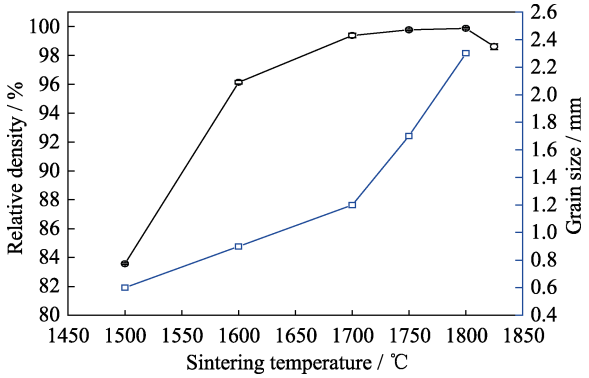

Fig. 7　Relative densities and average grain sizes of the 5at%Yb:YAG ceramics sintered at various temperatures for 20 h

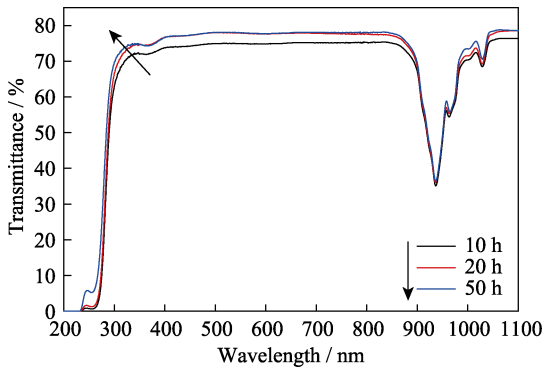

Fig. 8　In-line transmission curves of the 5at%Yb:YAG ceramics (2.2 mm thickness) sintered at 1800 ℃ for various holding time

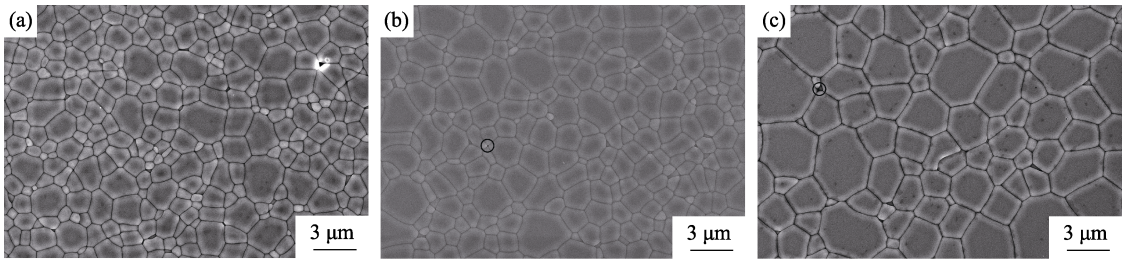

Fig. 9 FESEM micrographs of the thermally-etched surfaces of Yb:YAG ceramics sintered at 1800 ℃ for various holding time: (a) 10 h, (b) 20 h, (c) 50 h

with the in-line transmittance of those two ceramic samples in Fig. 8. In addition, there are still a few nano-sized pores at triple junctions or along grain boundaries in the ceramics sintered for 20 and 50 h, which act as optical scattering centers to degrade optical quality, so the in-line transmittance of ceramics is lower than the theoretical value of Yb:YAG ceramics.

The absorption and emission cross sections of the 5at%Yb:YAG ceramic at room temperature calculated from the in-line transmittance are shown in Fig. 10. The absorption cross section (σ_{abs}) can be calculated by the following equations:

$$R = \frac{(1-n)^2}{(1+n)^2} \tag{5}$$

$$T = \frac{(1-R)^2\exp(-\alpha b)}{1-R^2\exp(-2\alpha b)} \tag{6}$$

$$\sigma_{abs} = \frac{\alpha}{N} \tag{7}$$

$$N = \frac{\rho \times N_A}{M} \times C_s \tag{8}$$

Where n is the refractive index; R is the Fresnel reflectivity; the α and b are the absorption coefficient and the thickness of the ceramic sample, respectively; T is the in-line transmittance of the 5at%Yb:YAG ceramics obtained by the spectrophotometer; ρ is the theoretical density of the 5at%Yb:YAG ceramics (4.66 g/cm^3), N_A is the Avogadro's constant, M is molar mass, C_S is the doping concentration; N is the Yb^{3+} ions concentration of the 5at%Yb:YAG ceramics, which is 6.933×10^{20} ions/cm^3. The absorption cross section curve reveals that there are three main peaks/bands which locate at about 937, 965 and 1029 nm, respectively, and they are assigned to the radiation transition of the Yb^{3+} ions from the low $^2F_{7/2}$ to the high $^2F_{5/2}$ energy level. The main absorption cross section at 937 nm is 5.03×10^{-21} cm^2, which is smaller than that reported by Tang, *et al*[9] (6.1×10^{-21} cm^2 at 940 nm).

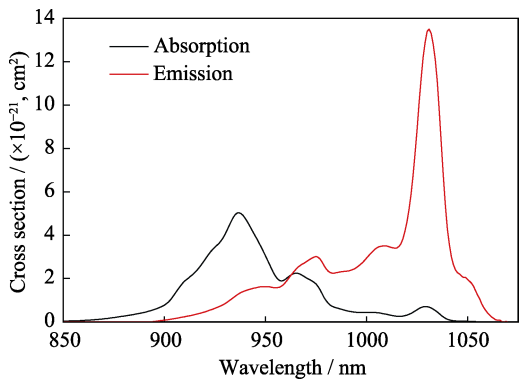

Fig. 10 Absorption and emission cross sections of the 5at%Yb:YAG ceramic sintered at 1800 ℃ for 50 h

Based on the absorption cross sections, the emission cross sections can be calculated by the reciprocity method shown as the following formula:

$$\sigma_{em}(\lambda) = \sigma_{abs}(\lambda)\frac{Z_l}{Z_u}\exp\left(\left(\frac{hc}{kT}\right)\left(\frac{1}{\lambda_{ZL}}-\frac{1}{\lambda}\right)\right) \tag{9}$$

$$Z_a = \sum_i d_i^a \exp\left(-\frac{E_i^a}{k_B T}\right) \tag{10}$$

Where Z_l and Z_u are partition function of the lower and upper energy levels, respectively. The formula (10) and energy levels can be used to calculate Z_l and Z_u, and then Z_l/Z_u can be obtained with a value of 0.88; h is the Planck constant of $6.62606896(33)\times10^{-34}$ J·s; c is light speed of 3.0×10^8 m/s; k is the Boltzmann constant of $1.3806505(24)\times10^{-23}$ J/K; the Kelvin's temperature, T, is chosen as 300 K; λ_{ZL} is the wavelength of the zero phonon line, which locate at 968 nm for the 5at%Yb:YAG ceramics at room temperature (300 K). Five peaks/bands can be found from the emission cross section curve at 949, 975, 1009, 1031 and 1049 nm, respectively. In addition, the main peak locates at about 1031 nm, and the value is 13.48×10^{-21} cm^2, which is smaller than that reported by Tang, *et al*[9] (19×10^{-21} cm^2 at 1030 nm).

According to the absorption and emission cross sections, the gain cross sections can be calculated by the following equation:

$$\sigma_g(\lambda) = \beta\sigma_{em}(\lambda) - (1-\beta)\sigma_{abs}(\lambda) \tag{11}$$

Where β is the particle inversion number. The gain cross sections calculated with different β are shown in Fig. 11. The smallest value of β is 0.048. Besides, when β is higher

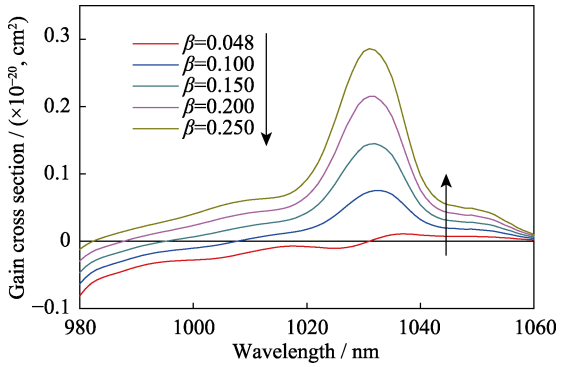

Fig. 11 Gain cross sections of the 5at%Yb:YAG ceramic sintered at 1800 ℃ for 50 h

than 0.048, the strongest peak locates at 1031 nm, which indicates that the laser would be generated at 1031 nm during the free laser test.

3 Conclusion

In this work, 5at%Yb:YAG precursors were synthesized *via* the co-precipitation method using pure water and alcohol-water mixture as the solvents, respectively. The powders were obtained by calcining precursors at 1250 ℃ for 4 h. And the average particle sizes of the powders with pure water and alcohol-water solvents are 174 and 133 nm, respectively. Compared to the powder with pure water solvent, the powder with alcohol-water solvent exhibits the same composition, smaller average crystallite size and lower agglomeration degree. Transparent 5at%Yb:YAG ceramics with alcohol-water solvent were fabricated by vacuum sintering without sintering additives. The ceramic sample sintered at 1800 ℃ for 50 h exhibits the highest in-line transmittance of 78.6% at 1100 nm and 76.7% at 400 nm (2.2 mm thickness). Concerning the spectroscopic properties, the absorption cross section at 937 nm is 5.03×10^{-21} cm^2, while the calculated emission cross section at 1031 nm is 13.48×10^{-21} cm^2. In our following work, the appropriate alcohol-water ratio will be optimized to further improve the dispersity of Yb:YAG powders, and the sintering strategy and the annealing process will be investigated to enhance the optical quality of Yb:YAG transparent ceramics.

References:

[1] IKESUE A, KINOSHITA T, KAMATA K, *et al*. Fabrication and optical properties of high performance polycrystalline Nd:YAG ceramics for solid-state lasers. *Journal of the American Ceramic Society*, 1995, **78(4):** 1033–1040.

[2] MESSING G L, STEVENSON A J. Toward pore-free ceramics. *Science*, 2008, **322(5900):** 383–384.

[3] IKESUE A, AUNG Y L, TAIRA T, *et al*. Progress in ceramic lasers. *Annual Review of Materials Research*, 2006, **36:** 397–429.

[4] WANG Z J, ZHOU G H, JIANG D Y, *et al*. Recent development of $A_2B_2O_7$ system transparent ceramics. *Journal of Advanced Ceramics*, 2018, **7(4):** 289–306.

[5] WEI J B, TOCI G, PIRRI A, *et al*. Fabrication and property of Yb:CaF_2 laser ceramics from co-precipitated nanopowders. *Journal of Inorganic Materials*, 2019, **34(12):** 1341–1348.

[6] KRELL A, WAETZIG K, KLIMKE J. Influence of the structure of $MgO{\cdot}nAl_2O_3$ spinel lattices on transparent ceramics processing and properties. *Journal of the European Ceramic Society*, 2012, **32:** 2887–2898.

[7] FEDOROV P P, OSIKO V V, KUZNETSOV S V, *et al*. Fluoride laser nanoceramics. *Journal of Physics: Conference Series*, 2012, **345:** 1–21.

[8] LUPEI V, LUPEI A, IKESUE A. Transparent polycrystalline ceramic laser materials. *Optical Materials*, 2008, **30(11):** 1781–1786.

[9] TANG F, CAO Y, GUO W, *et al*. Fabrication and laser behavior of the Yb:YAG ceramic microchips. *Optical Materials*, 2011, **33(8):** 1278–1282.

[10] ESPOSITO L, COSTA A L, MEDRI V. Reactive sintering of YAG-based materials using micrometer-sized powders. *Journal of the European Ceramic Society*, 2008, **28(5):** 1065–1071.

[11] MAITRE A, SALLE C, BOULESTEIX R, *et al*. Effect of silica on the reactive sintering of polycrystalline Nd:YAG ceramics. *Journal of the American Ceramic Society*, 2008, **91(2):** 406–413.

[12] STEVENSON A J, KUPP E R, MESSING G L. Low temperature, transient liquid phase sintering of B_2O_3-SiO_2-doped Nd:YAG transparent ceramics. *Journal of Materials Research*, 2011, **26(9):** 1151–1158.

[13] LEE S H, KOCHAWATTANA S, MESSING G L, *et al*. Solid-state reactive sintering of transparent polycrystalline Nd:YAG ceramics. *Journal of the American Ceramic Society*, 2006, **89(6):** 1945–1950.

[14] LI J, LIU J, LIU B L, *et al*. Influence of heat treatment of powder mixture on the microstructure and optical transmission of Nd:YAG transparent ceramics. *Journal of the European Ceramic Society*, 2014, **34(10):** 2497–2507.

[15] LI X X, WANG W J, HU Z G. Preparation of uniformly dispersed YAG ultrafine powders by coprecipitation method with SDS treatment. *Powder Metallurgy and Metal Ceramics*, 2009, **48(7/8):** 413–418.

[16] LI X, LIU H, WANG J Y, *et al*. Preparation and properties of YAG nano-sized powder from different precipitating agent. *Optical Materials*, 2004, **25(4):** 407–412.

[17] WANG Q Q, SHI Y, FENG Y G, *et al*. Li J. Spectral characteristics and laser parameters of solar pumped Cr,Nd:YAG transparent ceramics. *Chinese Journal of Luminescence*, 2019, **40(11):** 1365–1372.

[18] STEVENSON A J, LI X, MARTINEZ M A, *et al*. Effect of SiO_2 on densification and microstructure development in Nd:YAG transparent ceramics. *Journal of the American Ceramic Society*, 2011, **94(5):** 1380–1387.

[19] KWON O H, MESSING G L. A theoretical analysis of solution-precipitation controlled densification during liquid phase sintering. *Acta Metallurgica et Materialia*, 1991, **39(9):** 2059–2068.

[20] IKESUE A, KAMATA K. Microstructure and optical properties of hot isostatically pressed Nd:YAC ceramics. *Journal of the American Ceramic Society*, 1996, **79(7):** 1927–1933.

[21] JIANG N, OUYNAG C, LIU Y, *et al*. Effect of air annealing on the optical properties and laser performance of Yb:YAG transparent ceramics. *Optical Materials*, 2019, **95:** 109203.

[22] IKESUE A, YOSHIDA K, YAMAMOTO T, *et al*. Optical scattering centers in polycrystalline Nd:YAG laser. *Journal of the American Ceramic Society*, 1997, **80(6):** 1517–1522.

[23] KUPP E R, KOCHAWATTANA S, LEE S H, *et al*. Particle size effects on yttrium aluminum garnet (YAG) phase formation by solid-state reaction. *Journal of Materials Research*, 2014, **29(19):** 2303–2311.

[24] YANG L, LU T C, XU H, *et al*. Synthesis of YAG powder by the modified Sol-Gel combustion method. *Journal of Alloys and Compounds*, 2009, **484(1/2):** 449–451.

[25] SONG J G, PANG C L, CHEN L, *et al*. Preparation and properties of porous ceramics using YAG powder by hydrothermal precipitation method. *Journal of Synthetic Crystals*, 2018, **47(2):** 343–347.
[26] ZHANG X D, LIU H, HE W, *et al*. Novel synthesis of YAG by solvothermal method. *Journal of Crystal Growth*, 2005, **275(1/2):** E1913–E1917.
[27] LI J, PAN Y B, QIU F G, *et al.* Synthesis of nanosized Nd:YAG powders *via* gel combustion. *Ceramics International*, 2007, **33(6):** 1047–1052.
[28] MA B Y, ZHANG W, SHEN B Z, *et al.* Preparation and characterization of highly transparent Nd:YAG/YAG composite ceramics. *Optical Materials*, 2018, **79:** 63–71.
[29] SANG Y H, LIU H, SUN X D, *et al.* Formation and calcination temperature-dependent sintering activity of YAG precursor synthesized via reverse titration method. *Journal of Alloys and Compounds*, 2011, **509(5):** 2407–2413.
[30] SUN L N, ZHAO M S, TAN J, *et al.* Preparation of co-doped Ce,Pr:GAGG powder by chemical co-precipitation method and luminescence properties. *Chinese Journal of Luminescence*, 2019, **40(2):** 137–142.
[31] JING W, LI F, YU S Q, *et al.* High efficiency synthesis of Nd:YAG powder by a spray co-precipitation method for transparent ceramics. *Journal of the European Ceramic Society*, 2018, **38(5):** 2454–2461.
[32] LIU Q, Chen C, DAI J W, *et al*. Effect of ammonium carbonate to metal ions molar ratio on synthesis and sintering of Nd:YAG nanopowders. *Optical Materials*, 2018, **80:** 127–137.
[33] LI J G, IKEGAMI T, LEE J H, *et al.* Co-precipitation synthesis and sintering of yttrium aluminum garnet (YAG) powders: the effect of precipitant. *Journal of the European Ceramic Society*, 2000, **20(14/15):** 2395–2405.
[34] LI X Y, LIU Q, HU Z W, *et al*. Influence of ammonium hydrogen carbonate to metal ions molar ratio on co-precipitated nanopowders for TGG transparent ceramics. *Journal of Inorganic Materials*, 2019, **34(7):** 791–796.
[35] TONG S H, LU T C, GUO W. Synthesis of YAG powder by alcohol-water co-precipitation method. *Materials Letters*, 2007, **61(21):** 4287–4289.
[36] TONG S H, LU T C, GUO W, *et al.* Sinterability of Nd:YAG powder prepared by alcohol-water co-precipitation method. *Key Engineering Materials*, 2008, **368–372:** 423–425.
[37] CHEN X T, WU Y Q, WEI N, *et al*. Fabrication, photoluminescence and terahertz absorption properties of Yb:YAG transparent ceramics with various Yb dopant concentrations. *Optical Materials*, 2018, **85:** 106–112.
[38] CHEN X T, LU T C, WEI N, *et al.* Fabrication and microstructure development of Yb:YAG transparent ceramics from co-precipitated powders without additives. *Journal of the American Ceramic Society*, 2019, **102(12):** 7154–7167.
[39] RAHMANI M, MIRZAEE O, TAJALLY M, *et al*. Comparison of synthesis and spark plasma sintering of YAG nano particles by variation of pH and precipitator agent. *Ceramics International*, 2018, **44(18):** 23215–23225.
[40] SINGH G, RESHMA S S, SELVAMANI R, *et al.* Investigations on vacuum sintered ytterbium-doped YAG ceramic: a laser-host material. *Bulletin of Materials Science*, 2019, **42(6):** 273.
[41] CHEN X T, WU Y Q, WEI N, *et al.* The roles of cation additives on the color center and optical properties of Yb:YAG transparent ceramic. *Journal of The European Ceramic Society*, 2018, **38(4):** 1957–1965.

醇水共沉淀法制备 Yb:YAG 透明陶瓷及其性能研究

黄新友[1], 刘玉敏[1,2], 刘 洋[3], 李晓英[2,4], 冯亚刚[2,4], 陈肖朴[2,4], 陈鹏辉[1,2], 刘 欣[2,4], 谢腾飞[2,4], 李 江[2,4]

(1. 江苏大学 材料科学与工程学院, 镇江 212013; 2. 中国科学院 上海硅酸盐研究所, 透明光功能无机材料重点实验室, 上海 201899; 3. 华北光电技术研究所 固体激光科学与技术实验室, 北京 100015; 4. 中国科学院大学 材料与光电研究中心, 北京 100049)

摘 要: Yb:YAG 透明陶瓷由于具有宽的吸收带和发射带、高增益、低的热负载、长的荧光寿命、高的量子效率等优点而成为有应用前景的高功率固体激光器用增益介质。本研究优化了粉体的性能并制备了高透明的 Yb:YAG 陶瓷。以碳酸氢铵为沉淀剂, 分别以纯水或乙醇/水混合物为溶剂, 采用共沉淀法合成了 5at%Yb:YAG 纳米粉体。在 1250 ℃下煅烧 4 h 得到的所有粉体均为纯 YAG 相。与纯水溶剂制备的粉体相比, 醇水溶剂制备的粉体具有更小的平均晶粒尺寸和更低的团聚程度。以醇水溶剂制备的粉体为原料, 采用真空烧结法在不添加烧结助剂的情况下成功制备了 5at%Yb:YAG 透明陶瓷, 并对 1500~1825 ℃烧结 20 h 和 1800 ℃烧结 10~50 h 所得陶瓷的微观结构和直线透过率进行了探究。除在 1825 ℃下烧结 20 h 所得的陶瓷外, 其余的 5at%Yb:YAG 陶瓷都具有均匀的微观结构。在 1800 ℃下烧结 50 h 制备的 5at%Yb:YAG 陶瓷具有最高的光学质量, 在 1100 和 400 nm 处的直线透过率分别为 78.6%和 76.7%(样品厚度为 2.2 mm)。该 Yb:YAG 透明陶瓷在 937 nm 处的吸收截面为 5.03×10^{-21} cm^2, 在 1031 nm 处的发射截面为 13.48×10^{-21} cm^2。

关 键 词: Yb:YAG 透明陶瓷; 醇水共沉淀法; 真空烧结; 微观结构; 光学性能

中图分类号: TQ174 **文献标识码:** A